

BOND ENERGY OF ADSORBED AND INTERLAYER WATER: KEROLITE DEHYDRATION AT ELEVATED PRESSURES

ANNA KOKINES MILLER, STEPHEN GUGGENHEIM, AND AUGUST F. KOSTER VAN GROOS

Department of Geological Sciences, University of Illinois at Chicago
Chicago, Illinois 60680

Abstract—The dehydration reaction of kerolite was investigated using high-pressure differential thermal analysis at pressures as high as 600 bars. The peak associated with the dehydration is broad, suggesting the presence of a series of overlapping reactions ranging from the release of adsorbed water to interlayer water. The peak temperature is 136°C at 1.8 bars and increases to 516°C at 586 bars. The primary reaction represents loss of adsorbed water having a bond energy of 1.5 ± 1 kJ/mole. A small amount of water may be present as interlayer water and has a bond energy of 7.5 ± 3 kJ/mole.

Key Words—Bond energy, Dehydration, High-pressure differential thermal analysis, Kerolite, Water.

INTRODUCTION

Kerolite (approximately $\text{Mg}_3\text{Si}_4\text{O}_{10}(\text{OH})_2 \cdot n\text{H}_2\text{O}$, where $n = 0.8\text{--}1.2$) is a fine-grained phyllosilicate having an apparent basal spacing of 10.0 Å; it is characterized by slight swelling in ethylene glycol (Brindley and Pham Thi Hang, 1973; Brindley *et al.*, 1977). Kerolite forms at low temperatures and is commonly mixed with either stevensite or serpentine. It occurs with carbonates as an alteration product of sepiolite or possibly as a direct precipitate from ground water having a pH < 8 (Stoessel and Hay, 1978; Hay and Stoessel, 1984). Dissolution experiments by Stoessel (1988) showed that kerolite is metastable relative to sepiolite in saturated silica solutions at surface conditions. Eberl *et al.* (1982) and Khoury *et al.* (1982) described mixed-layer stevensite/kerolite that appeared to have precipitated from saline solutions and that was possibly a precursor in the secondary formation of sepiolite. Kerolite also occurs in weathering profiles of ultramafic igneous rocks (Maksimović, 1966; Brindley *et al.*, 1977).

Brindley *et al.* (1977) found the actual basal spacing of kerolite to be 9.65 Å, after correction for Lorentz-polarization effects. Most of the increase in the basal spacing compared with that of talc (9.38 Å) was attributed to disordered layer stacking, which produced less effective packing along Z^* . They argued that the presence of H_2O in the interlayer was not responsible for the increase in the basal spacing. Brindley *et al.* (1977) found that weight loss due to dehydration was gradual between 110° and 700°C. The dehydration was completely reversible after heating to 300°C and 70–90% reversible after heating to 650°C. On the basis of the gradual weight loss, its variable rehydration potential, and infrared (IR) data showing several frequencies attributed to molecular water and hydroxyl groups, they speculated that water in kerolite could reside in a number of locations, such as layer surfaces and edges. They suggested that most of the water was present as

adsorbed molecular water and as surface hydroxyls, with a small amount possibly retained in the hexagonal rings of the tetrahedral sheet.

As noted by Brindley *et al.* (1977), kerolite is distinguished from talc by the extreme disorder of the layer stacking and its greater ability to hold H_2O molecules and OH ions at surface imperfections. This behavior is similar to that of smectite; however, the non-swelling behavior of kerolite offers the opportunity to study the effects of surface properties, without interference of an expanding interlayer region. In the present study, the bonding of these surface molecules was investigated by high-pressure differential thermal analysis (HP-DTA). We show below that the bond energy for adsorbed water may be distinguished from that of interlayer water.

EXPERIMENTAL METHODS

Apparatus

The DTA apparatus has been described previously (Koster van Groos, 1979). In short, it consists of a Cu sample holder for two samples and a reference ($\alpha\text{-Al}_2\text{O}_3$), placed in Au capsules, which are open or welded shut. The capsules weigh about 120 mg each, and are 7–8 mm long, 3 mm in diameter, and have 0.7-mm-thick walls. A 1-mm re-entry well at the bottom of the capsule accommodates a Pt/Pt₉₀Rh₁₀ thermocouple. The sample holder is placed inside an internally heated pressure vessel (IHPV) similar to that described by Holloway (1971). Temperature was measured by the reference thermocouple and corrected using the differential temperature. Quartz was added to each sample to calibrate temperature, using the low-high quartz transition; correction factors were typically 1°–2°C. Temperature signals were recorded on the 20- μV or 50- μV range of a Kipp-Zonen recorder; the resulting resolution was 0.02°–0.05°C. The heating rate of all runs was 20°C/min, using a Honeywell programmable controller. Argon was the pressure medium; pressures

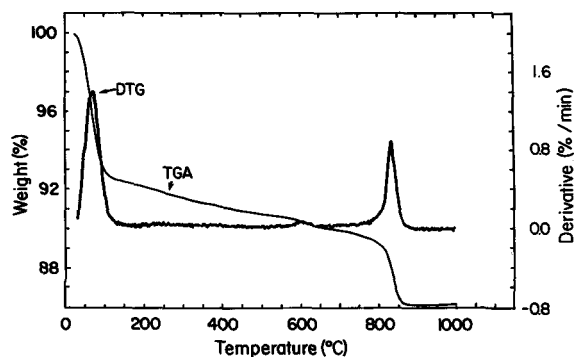


Figure 1. Thermogravimetric data for kerolite (after Evans and Guggenheim, 1988).

were measured using calibrated, high-precision Bourdon-type pressure gauges for low-, medium-, and high-pressure ranges.

The samples were also analyzed (Figure 1) by thermogravimetric and differential thermogravimetric analysis (TGA, DTG) through the courtesy of P. van der Krieken at the Instituut voor Aardwetenschappen, University of Utrecht, The Netherlands. The samples were run in an anhydrous N_2 atmosphere using a DuPont 1090 analyzer.

Starting materials

The kerolite used in this study was from Carter's Mine, Madison County, North Carolina, and was described by Brindley *et al.* (1977). Individual crystallites are plates about 150 Å in diameter in plan. They were mineralogically pure, but contained trace amounts of Ca^{2+} , Na^+ , and K^+ . The sample was mixed with 20 wt. % quartz (St. Peters sandstone ground to <200 mesh) and stored at 55% relative humidity over a saturated $Mg(NO_3)_2 \cdot H_2O$ solution.

Experimental procedure

Samples weighing 16–20 mg were run in open and sealed capsules. To reduce argon and H_2O gas mixing and to maintain $P(\text{total}) = P(H_2O)$ within the sample, the open capsules were packed with silica wool. Initially, several runs were made with water added to the starting material, but the boiling peak of water interfered with the dehydration reaction. Therefore, all the runs reported here were made without additional water. The sealed capsules were checked for leaks and weighed before and after the experiment. Those that lost weight were discarded. Run products were analyzed with Cu radiation by the Debye-Scherrer powder X-ray diffraction method.

RESULTS AND DISCUSSION

Figure 1 shows a TGA and a DTG of kerolite. Two well-defined weight-loss events were encountered. The first event (hereafter referred to as "dehydration"), at 75°C, marked a rapid loss of as much as 8 wt. % ad-

Table 1. Pressure and temperature data for the kerolite dehydration reaction.

Pressure (bars)	Extrapolated onset temperature (°C)	Peak temperature (°C)	Extrapolated return temperature (°C)
1.8	117	136	164
11	178	205	231
60 ¹	275	287	316
150	231	319	368
154 ¹	345	363	380
327 ¹	389	432	461
328	305	340	410
586 ¹	384	516	560

¹ Indicates closed-capsule runs.

sorbed and, possibly, any interlayer water. An additional 3 wt. % water was lost gradually until the second rapid weight-loss at about 830°C. This latter event corresponded to the dehydroxylation of the 2:1 layers, comparable to the dehydroxylation of talc, although the temperature was slightly less than that of talc. Note that this analysis was made at $P(H_2O) \ll 1$ atm, and the temperatures cannot be compared directly with results obtained at $P(H_2O) = 1$ atm.

Nine open-capsule and twelve closed-capsule runs were made in the HP-DTA study. Four open-capsule

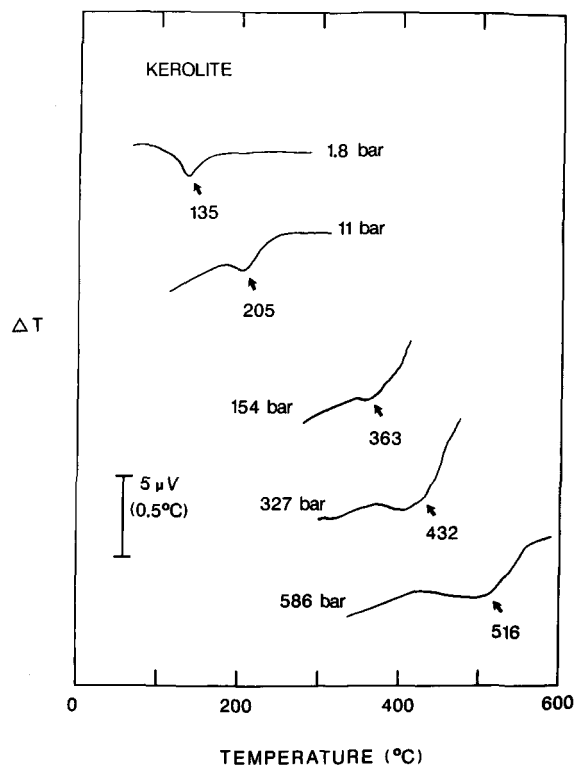


Figure 2. High-pressure differential thermal analysis curves of the kerolite dehydration reaction at different pressures. Curves at pressures labelled 1.8 and 11 bar are open-capsule experiments; the others are closed-capsule runs. Arrows indicate peak temperature.

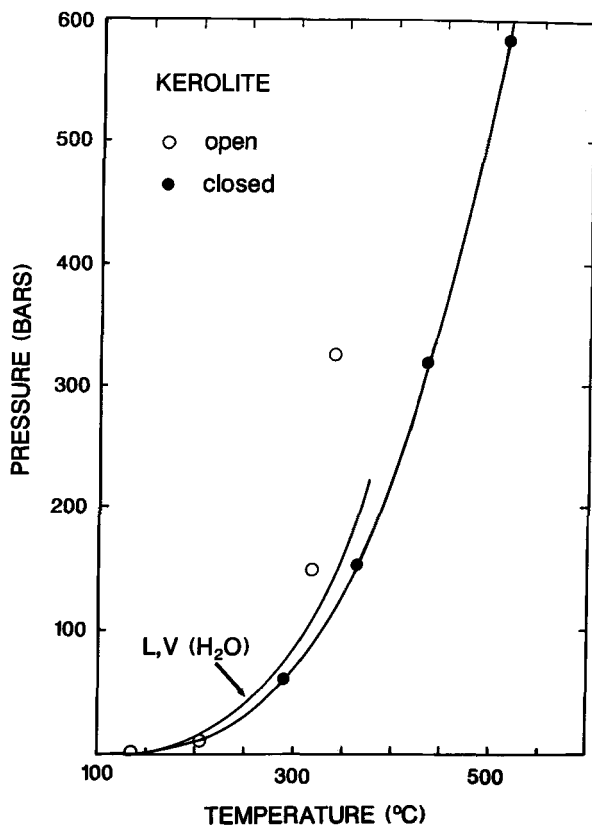


Figure 3. Pressure and temperature relations of the kerolite dehydration. The boiling reaction of water, L,V (H₂O) is shown for comparison (Keenan *et al.*, 1978).

and four closed-capsule runs were successful. Table 1 lists the extrapolated onset temperature, which represents the intersection of the tangent of the main slope of the peak at its low temperature side; the peak temperature, which is the temperature of maximum deviation from the base line; and the extrapolated return temperature, representing the intersection of the tangent of the main slope of the peak at the high-temperature side with the base line; for the dehydration reaction for kerolite. Figure 2 shows the HP-DTA results from two selected open-capsule and three closed-capsule runs. Note that all peaks in the patterns are broad, indicating that either P(H₂O) increased during dehydration (Koster van Groos and Guggenheim, 1984) or that the dehydrating H₂O was bonded or adsorbed at significantly different locations in or on the crystallites to produce several thermal events represented by a single broad peak. Except at temperatures above the critical point of water, increased pressure had no apparent effect on peak shape. Above the critical point of water, however, the dehydration peak appears to have occurred over a wider temperature range.

Peak temperatures and the boiling curve of water are shown in P-T space in Figure 3. Because the molar volume of water is very high at low pressures, evolving

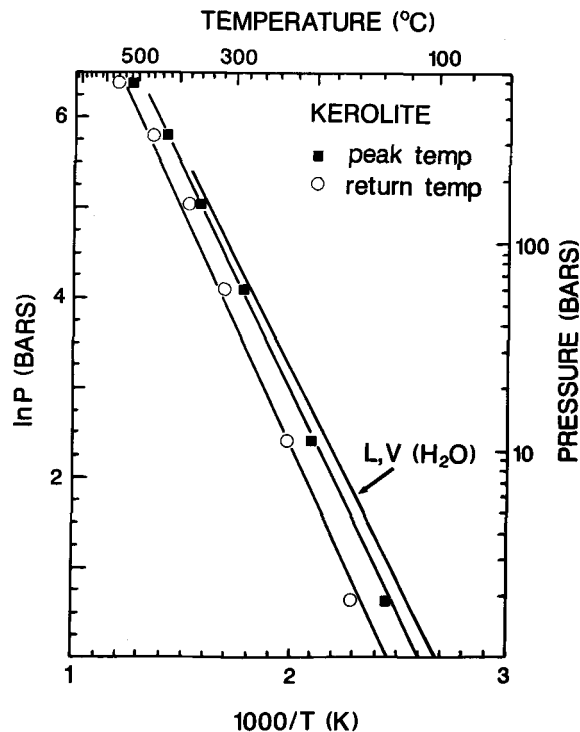


Figure 4. Kerolite dehydration peak-temperatures and extrapolated return temperatures as a function of $\ln P$ vs. $1000/T$ (K). The boiling reaction of water, L,V (H₂O), is shown for comparison.

H₂O gas probably flushed any Ar gas from the open-capsule runs at 1.8 and 11 bars. Hence, both the low-pressure open-capsule and all the closed-capsule peak temperatures were obtained with $P(\text{total}) = P(\text{H}_2\text{O})$. The consistency (Figure 3) of the plotted open-capsule low-pressure runs and the closed-capsule runs supports this assumption. The dehydration curve of kerolite is located near the boiling curve of water, indicating that water associated with kerolite behaved similarly to unbound water. The results, therefore, suggest that most of the water present is adsorbed molecular water.

Dehydration peak and return temperatures are shown in the $\ln P$ vs. $1000/T$ plot in Figure 4. The data define straight lines, the slopes of which represent an expression of the molar enthalpy of dehydration ΔH_{dh} , following the Clausius-Clapeyron equation, $d \ln P/dT = \Delta H_{\text{dh}}/RT^2$, and the assumption that the fugacity coefficient $\Gamma_{\text{H}_2\text{O}} = 1$ and that the heat capacity ΔC_p of the participating solid phases is zero (e.g., see Anderson, 1977). The enthalpy determined includes the enthalpy of evaporation of the adsorbed and interlayer water. Therefore, the enthalpy of the bond was calculated by subtracting the enthalpy of evaporation of water (Koster van Groos and Guggenheim, 1986). This procedure yields the bond enthalpy of the adsorbed water, $\Delta H_{\text{ads.water}} = 1.5 \pm 1$ kJ/mole. This value represents the difference in slope between the dehydration reaction

and the boiling reaction of water. Because the broad peak represents several thermal events (see above), the last dehydration reaction probably occurred near the temperature at which the DTA dehydration signal returns to the base line (extrapolated return temperature). The extrapolated return temperatures are shown in Figure 4; the enthalpy associated with this reaction, after subtraction of the enthalpy of the evaporation of water at the dehydration temperature, is $\Delta H = 7.5 \pm 3$ kJ/mole. This value is similar to the enthalpy values (7.8–12.1 kJ/mole) reported for cation-exchanged montmorillonite (Koster van Groos and Guggenheim, 1986, 1987). The interlayer-water enthalpy of the montmorillonite is probably related to the second nearest-neighbors to the interlayer (Na, K, Ca, Mg) cation; first nearest-neighbor hydration shells have enthalpy values that are considerably higher. Thus, the ΔH of 7.5 kJ/mole of kerolite appears to be a reasonable value for interlayer water in the silicate rings of a neutral 2:1 layer in the absence of an interlayer cation.

SUMMARY AND CONCLUSIONS

Most of the water associated with kerolite is weakly bonded (1.5 ± 1 kJ/mole) and is probably attracted to layer surfaces. A small amount of water is more strongly bonded (as much as 7.5 ± 3 kJ/mole) and is probably interlayer water. Although the analyses of Brindley *et al.* (1977) indicated a small amount of alkali cations in the interlayer, no evidence of a dehydration reaction similar to that observed in montmorillonite was noted here; however, the amount present was probably too small to be detected by the DTA system. Brindley *et al.* (1977) also suggested the presence of adsorbed OH, which would presumably have greater coulombic interaction than adsorbed water. No evidence for OH-loss was found by DTA, although the gradual weight-loss of about 3 wt. % between 75° and 830°C in the TGA data may be related to a series of reactions involving the loss of adsorbed OH.

ACKNOWLEDGMENTS

We thank D. L. Bish, Los Alamos National Laboratory, and R. L. Hay, University of Illinois, Urbana, for samples and F. A. Wicks, Royal Ontario Museum, and R. K. Stoessel, University of New Orleans, for reviews of the manuscript. Support for this research was provided by the Petroleum Research Fund of the American Chemical Society under grants 17263-AC2, 21974-AC8-C, and 20016-AC2 and by the National

Science Foundation under grants EAR-8704681 and EAR-8816898.

REFERENCES

- Anderson, G. M. (1977) Fugacity, activity and equilibrium constant: in *Application of Thermodynamics to Petrology and Ore Deposits*, H. J. Greenwood, ed., Mineralogical Association of Canada Short Course Handbook 2, 17–37.
- Brindley, G. W. and Pham Thi Hang (1973) The nature of garnierite-I. Structures chemical compositions and color characteristics: *Clays & Clay Minerals* **19**, 27–40.
- Brindley, G. W., Bish, D. L., and Wan, H. (1977) The nature of kerolite; its relation to talc and stevensite: *Mineral. Mag.* **41**, 443–452.
- Eberl, D. D., Jones, B. F., and Khoury, H. N. (1982) Mixed-layer kerolite/stevensite from the Amargosa Desert, Nevada: *Clays & Clay Minerals* **30**, 321–326.
- Evans, B. W. and Guggenheim, S. (1988) Talc, pyrophyllite and related minerals: in *Hydrous Phyllosilicates (Exclusive of Micas)*, S. W. Bailey, ed., *Reviews in Mineralogy* **19**, Mineralogical Society of America, Washington, D.C., 225–294.
- Hay, R. L. and Stoessel, R. K. (1984) Sepiolite in the Amboseli basin of Kenya: A new interpretation: in *Sepiolite and Palygorskite: Occurrences, Genesis and Uses*, A. Singer and E. Galan, eds., Elsevier, Amsterdam, 125–136.
- Holloway, J. R. (1971) Internally heated pressure vessels: in *Research for High Pressure and Temperature*, G. C. Ulmer, ed., Springer-Verlag, New York, 217–258.
- Keenan, J. H., Keyes, F. G., Hill, P. G., and Moore, J. G. (1978) *Steam Tables: Thermodynamic Properties of Water Including Vapor, Liquid, and Solid Phases*: Wiley, New York, 156 pp.
- Khoury, H. N., Eberl, D. D., and Jones, B. F. (1982) Origin of the clays from the Amargosa Desert, Nevada: *Clays & Clay Minerals* **30**, 327–336.
- Koster van Groos, A. F. (1979) Differential thermal analysis in the system NaF–Na₂CO₃ to 10 kbar: *J. Phys. Chem.* **83**, 2976–2978.
- Koster van Groos, A. F. and Guggenheim, S. (1984) The effect of pressure on the dehydration reaction of the interlayer water in Na-montmorillonite (SWy-1): *Amer. Mineral.* **69**, 872–879.
- Koster van Groos, A. F. and Guggenheim, S. (1986) Dehydration of K-exchanged montmorillonite at elevated temperatures and pressures: *Clays & Clay Minerals* **34**, 281–286.
- Koster van Groos, A. F. and Guggenheim, S. (1987) Dehydration of a Ca- and a Mg-exchanged montmorillonite (SWy-1) at elevated pressures: *Amer. Mineral.* **72**, 292–298.
- Maksimovič, Z. (1966) β -kerolite-pimelite series from Goles Mountain, Yugoslavia: in *Proc. Int. Clay Conf., Jerusalem, 1965, Vol. 1*, L. Heller and A. Weiss, eds., Israel Program for Scientific Translations, Jerusalem, 97–105.
- Stoessel, R. K. and Hay, R. L. (1978) The geochemical origin of sepiolite and kerolite from Amboseli, Kenya: *Contr. Mineral. Petr.* **65**, 255–267.
- Stoessel, R. K. (1988) 25°C and 1 atm dissolution experiments of sepiolite and kerolite: *Geochim. Cosmochim. Acta* **52**, 365–374.

(Received 23 March 1990; accepted 30 June 1990; Ms. 1993)